Petroleum Science xxx (xxxx) xxx

Contents lists available at ScienceDirect

Petroleum Science

journal homepage: www.keaipublishing.com/en/journals/petroleum-science

Short Communication

Evaluating hydraulic fracturing effectiveness based on the improved connection model of acoustic emission events

Shan Wu [a,*], Hong-Kui Ge [c], Xiao-Qiong Wang [c], Ke Gao [b,**], Hai Ding [d]

[a] School of Resources and Environmental Engineering, Hefei University of Technology, Hefei, 230009, Anhui, China
[b] Department of Earth and Space Sciences, Southern University of Science and Technology, Shenzhen, 518000, Guangdong, China
[c] State Key Laboratory of Petroleum Resources and Prospecting, China University of Petroleum (Beijing), Beijing, 102249, China
[d] Exploration Research Institute, Anhui Provincial Bureau of Coal Geology, Hefei, 230088, Anhui, China

ARTICLE INFO

Article history:
Received 16 February 2025
Received in revised form
22 July 2025
Accepted 23 July 2025
Available online xxx

Edited by Jia-Jia Fei

Keywords:
Fracturing effectiveness
Connection model
True tri-axial experiment

ABSTRACT

Hydraulic fracturing techniques are commonly used to enhance the production of tight reservoirs. Generally, the effect of hydraulic fracturing can be appraised through hydraulic fracturing experiments in the laboratory, in which acoustic emission (AE) is often used to monitor the fracturing process. At present, the number of AE events and spatial distribution of AE locations are the two main factors commonly considered in hydraulic fracturing effectiveness evaluation. However, these commonly used evaluation methods overlook two crucial aspects: the connectivity among fractures and the tensile and shear properties of fractures induced by hydraulic fracturing. In this technical note, we consider the influence of these two previously overlooked aspects on the evaluation of hydraulic fracturing effectiveness by establishing a connected fracture model using AE data. The proposed approach links up AE events based on their spatio-temporal relationship and builds a fracture network called the connection model. Then, the characteristic of the fracture network is represented by the fractal dimension to reveal the complexity of fractures in the network. We extract the tensile-shear properties of each fracture based on the inversion of AE events' focal mechanism. Finally, based on the pre-known fracturing effectiveness of a fracture network, we compare the connection model of AE events in several triaxial hydraulic experiments. Our findings indicate that a comprehensive evaluation of hydraulic fracturing effectiveness can be achieved by considering both the connectivity of AE locations and the tensile-shear properties of AE events. This work aims to provide a more rational method for characterizing rock fracture networks and evaluating rock fracturing effects using AE data.

1. Introduction

Hydraulic fracturing is an essential technology for efficient production in low-permeability reservoirs (Warpinski et al., 2013). High-pressure fluids are injected into the reservoir to create new fractures or activate natural fractures. As a result, the permeability of a tight reservoir in large volume areas is improved (Gale et al., 2018; Taleghani et al., 2013), which is a direct reflection of the hydraulic fracturing effectiveness. Evaluating the fracturing effect is significant for optimizing hydraulic fracturing operations to enhance production.

To investigate the fracturing effect under controlled conditions, tri-axial hydraulic fracturing experiments that simulate the fracturing process in the field are often conducted with acoustic emission (AE) monitoring. As it is difficult to measure the fracturing effect (the improvement of permeability) directly, ranges of fractures induced by hydraulic fracturing can be an indicator to represent the fracturing effect (Wu et al., 2025). Typically, the range of fractures is determined by the envelope volume of AE locations, which is analogous to the application of microseismic events in field studies (Maxwell, 2011; Mayerhofer et al., 2010). However, the envelope volume can only roughly signify the spatial area of fractures represented by AE events rather than the detailed structures of fracture networks (Liu et al., 2018). Specifically, it cannot capture the degree of zigzagging in fractures or the

* Corresponding author.
** Corresponding author.
E-mail addresses: wus@hfut.edu.cn (S. Wu), gaok@sustech.edu.cn (K. Gao).
Peer review under the responsibility of China University of Petroleum (Beijing).

https://doi.org/10.1016/j.petsci.2025.07.018

complexity of fracture networks caused by branching. Since these two factors can significantly impact reservoir permeability after fracturing, a method that can accurately reflect the structure of fracture networks is essential for evaluating the fracturing effect.

To determine the structure of the fracture network, the first step is to establish the connections between dispersed AE events that merely represent the initiation of each fracture. The method of obtaining the complete structure of fractures through their initiation points has been a primary focus in the study of faults in seismology. Frohlich and Davis (1990) employed a single-link cluster (SLC) method to quantitatively measure the degree of clustering or isolation of seismic events to determine the migration process of seismic faults. Hugot et al. (2015) proposed a more advanced connection method based on the SLC method to link microseismic events from hydraulic fractures in the field. Hugot's approach considers the influence of in-situ stress, reservoir rock properties, and injection pressure on the connections between microseismic events. Although this new connection model has been applied to evaluate the effects of hydraulic fracturing using microseismic events in the field, its use in analyzing AE data for evaluating hydraulic fracturing effectiveness in laboratory settings is rare, and its applicability has not been fully discussed.

After constructing the connection model, the next step is to quantitatively characterize the structure of the fracture network. If the fracture network consists of simple planar fractures, it can be characterized by defining the length, width, and height. However, in unconventional reservoirs, hydraulic fracturing typically forms complex fracture networks. Quantitatively characterizing fracture networks with irregular three-dimensional geometries is still challenging. Fractal analysis provides a useful tool for describing such irregular shapes and quantifying the complexity of fracture networks (Zhang et al., 2017b). Lei (2019) employed the correlation dimension in fractal analysis to describe the process of rock rupture under uniaxial compression, showing that the nucleation of multiple fractures is accompanied by an increase in fractal dimension. Li et al. (2009) used the box dimension of fractal analysis to describe the spatial complexity of a three-dimensional fracture network. Applying fractal methods to the analysis of the connection model can enable a quantitative description and enhance the evaluation of the fracturing effect.

In addition to the structure of fracture networks, the tensile-shear mechanical properties of fractures impact the permeability of fractures as well and should also be considered in the evaluation of hydraulic fracturing effectiveness. Tensile fractures often have a certain degree of opening, which can greatly improve the permeability of fractures. However, shear fractures have limited capability to improve permeability (Auradou et al., 2005), and they can improve the permeability only when they form self-support between fracture surfaces (Wang et al., 2019). The tensile-shear mechanical properties of fractures can be obtained by inversion of the focal mechanism of AE. The simplified moment tensor inversion method proposed by Ohtsu (1995) is the most commonly used for such inversion, and it has been used in many experiments in rock mechanics. This method is based on the isotropic Green's field hypothesis, so it is commonly used in homogeneous rock/rock-like media such as cement, granite, and marble (Chang and Lee, 2004; Hampton et al., 2013; Manthei, 2005; Ohno and Ohtsu, 2010; Wang et al., 2017). In recent years, this method has also been used in rocks with strong heterogeneity, such as coal and shale. Results show that it performs well in assessing the tensile-shear properties of AE events with strong heterogeneity. Therefore, the simplified moment tensor inversion method can be used to determine the tensile-shear properties of AE events. The tensile-shear properties of fractures can be inferred from the tensile-shear properties of the AE events involved, as a single fracture typically contains multiple AE events.

In this paper, to better evaluate the hydraulic fracturing effectiveness, we utilize the connection model to analyze AE results in fracturing experiments considering both the structure of fracture network and the tensile-shear properties of fractures (Li et al., 2018b; Wu et al., 2019b). To validate the method, based on prior analyses of the fracturing effect, we compare the fractal dimension and the tensile-shear properties of a fracture network in different rocks. This paper is organized as follows. In Section 2, we introduce the establishment of the fracture connection model, fractal method, and the moment tensor decomposition for obtaining tensile-shear properties of fractures, and also present the experimental data used in this paper. In Section 3, we present the analysis results based on the connection model. Then, we discuss the fracturing effect evaluation method in Section 4 based on the connection model and conclude in Section 5.

2. Theory, method and data

2.1. The connection model of AE events

The connection model of fractures proposed by Hugot et al. (2015) is based on the time sequence and spatial correlation of AE events. The steps are demonstrated as follows.

(1) AE events are arranged in a time sequence forming a set ***M***. Each AE event is labeled as $P_M(x,y,z,t)$, where x, y, and z are the coordinates, and t denotes time.
(2) Define ***N*** as the set of AE events constituting the connected fracture network. Each AE event is labeled as $P_N(x,y,z,t)$. The connecting procedure involves transferring AE events from set ***M*** to ***N***. The initial point P_{N_0} in ***N*** is also the initial point P_{M_0} in ***M***.
(3) Denote the distance from point P_{M_i} to set ***N*** as $d(N, P_{M_i})$. There are two ways to define $d(N, P_{M_i})$: a) event-event, i.e., the distance from P_{M_i} to the AE events of ***N*** set (Fig. 1(a)); b) event-network, i.e., the distance from P_{M_i} to the fractures of ***N*** set (Fig. 1(b)).
(4) Connect P_{M_i} to the AE events with the smallest $d(N, PM_i)$, forming a new fracture segment.
(5) Repeat steps (1)–(4) until all AE events in ***M*** are connected to ***N***, resulting in a complete connected fracture network.

The connection model defines a branch number of fractures. Starting from the first fracture segment, when the fracture

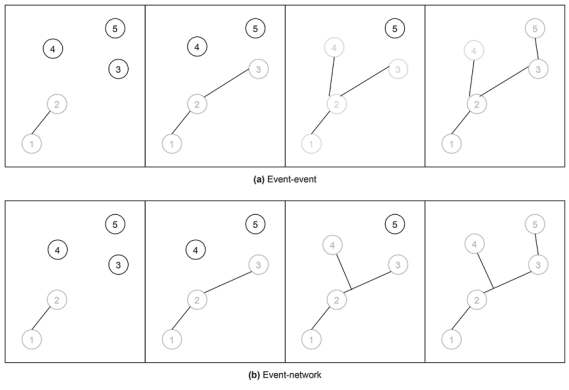

Fig. 1. The method for establishing models (modified from Hugot et al. (2015)).

segment branches, the branch number of the new fracture segment increases by one to the connected fracture segment. The branching number of the first fracture segment is 1, which is then accumulated, as shown in Fig. 2.

2.2. Fractal method

Hydraulic fracturing in shale and tight sandstone typically creates complex fracture networks characterized by irregular, three-dimensional geometries. Traditional geometric descriptors struggle to effectively quantify such complexities. Therefore, fractal dimension analysis, known for its ability to describe and quantify geometric irregularities and spatial heterogeneity, is employed here to better characterize the complexity of these fracture networks. The fractal dimension can be used to quantify the complexities of connection models, reflecting the degree of zigzagging. In this paper, we use the correlation dimension to quantify the fractal dimension (Lei, 2019). The calculation of the correlation dimension is (Kurths and Herzel, 1987)

$$C_q(r) = \frac{1}{n}\sum_{i=1}^{n}\left(\frac{n_i(R \le r)}{n-1}\right), \quad (1)$$

where R is the length of fractures in the connected model, and $n_i(R \le r)$ is the number of fractures with a length less than r. R reflects the length of links in the connection model, representing the distance between AE events. The correlation dimension shows the spatial distribution between fractures. If the correlation dimension number is small, the propagation of fractures has a small-scale span and thus yields a single-scale feature of the fracture network. A large correlation dimension indicates a multi-scale fracture network, reflecting a better fracturing effect that benefits oil and gas production in tight reservoirs.

2.3. Mechanical properties of fractures

The moment tensor contains the mechanical mechanism of AE events. Generally, the moment tensor of AE can be inverted by the polarity and amplitude of the P wave. Ohtsu (1991) first applied this method based on the simplified Green's function and proposed a procedure to decompose the moment tensor (Fig. 3). The AE events can be divided into three types: tensile, shear, and mixed. The components of the moment tensor reflect the tensile-shear properties of each AE event. Then, the mechanical property of each fracture in the connection model can be determined by the ratio of tensile and shear AE events.

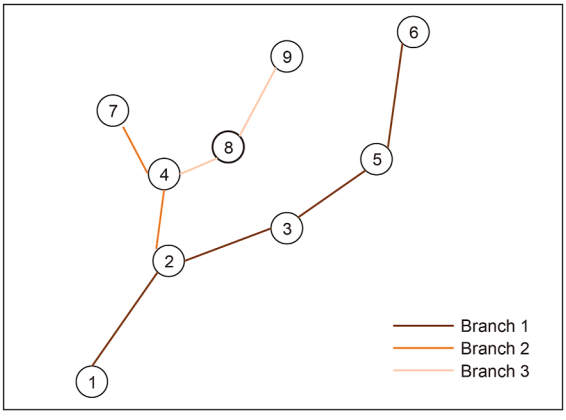

Fig. 2. Schematic diagram of the definition of branch number (modified from Hugot et al. (2015)).

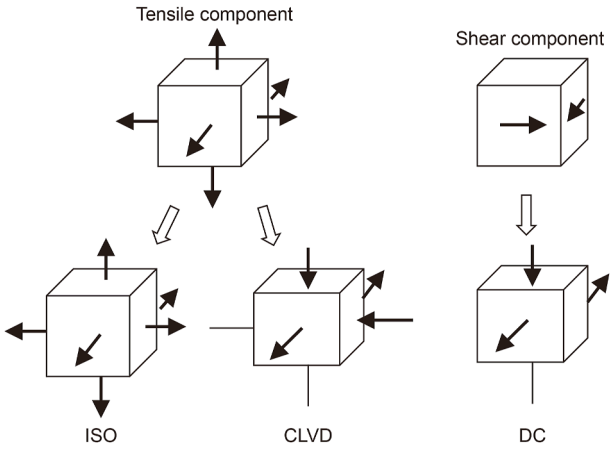

Fig. 3. The decomposition of moment tensor (modified from Ohtsu (1991)).

2.4. Experimental data and prior information

The hydraulic fracturing effectiveness is influenced by rock lithology, fracturing fluid viscosity, and injection rate. This study compares the hydraulic fracturing effectiveness on rock samples with two types of lithologies using various fracturing fluids. The experiments are conducted on a true triaxial fracturing simulation system, and the AE data are collected using the DS5 multi-channel continuous waveform monitoring equipment. A detailed introduction about the equipment can be found in the referenced papers (Li et al., 2018b; Wu et al., 2019a). The experimental parameters used in this paper are presented in Table 1, with some of them sourced from published experiment data. We relabel the samples and also provide their labels from the original paper. The AE data from these experiments are employed to re-analyze the hydraulic fracturing effectiveness based on the connection model.

As indicated in Table 1, the results of C7_1, C7_2, and LMX_1 reflect the influence of lithology on the hydraulic fracturing effectiveness. According to previous studies, hydraulic fracturing forms a complex fracture network in shales; whereas in tight sandstone, it tends to form relatively simple fracture structures (Guo et al., 2015; Zou et al., 2018). The LMX_4 and LMX_SCO$_2$ can be used to compare the influence of different fracturing fluids. It is known that supercritical CO_2 can promote the formation of complex fractures (Ishida et al., 2016; Middleton et al., 2014; Zhang et al., 2017a), whereas X-linked guar tends to form fractures with simple shapes (Bennour et al., 2015; Ishida et al., 2004). The difference between LMX_2 and LMX_3 lies in the different σ_v, i.e., the vertical in-situ stress. Fig. 4 illustrates detailed CT scan results showing that complex fracture networks are formed in LMX_2, while relatively simple fractures are formed in LMX_3.

The above prior information above provides a qualitative comparison of the complexity of fracture networks in the samples. It is worth noting that fracture complexity is not necessarily equivalent to the effectiveness of hydraulic fracturing. Although currently there is no deterministic conclusion, many field data and numerical simulation analyses support the idea that complex fracture networks are generally associated with better fracturing. This paper does not intend to discuss such a relationship. Instead, we adopt the general recognition that more complex fracture networks represent a better fracturing effect. Therefore, the following prior information is used to verify the evaluation of hydraulic fracturing effectiveness based on the connection model in this paper:

Table 1
The experimental parameters of all the samples.

	Label of rock in the cited paper	Lithology	Stress state $\sigma_h/\sigma_H/\sigma_v$, MPa	Fracturing fluid	Injection rate, mL/min
C7_1	New data	Tight sandstone	10/15/25	Water	20
C7_2			10/15/25	Water	20
LMX_1	Specimen 2 (Li et al., 2018a)	Shale	10/15/25	Water	20
LMX_2	Specimen 1 (Li et al., 2018a)		10/15/30	Water	20
LMX_3	Specimen 4 (Li et al., 2018a)		10/15/15	Water	20
LMX_4	New data		10/15/25	X-linked guar	20
LMX_SCO$_2$	Shale_sc (Wu et al., 2019b)		10/15/25	Supercritical-CO$_2$	5

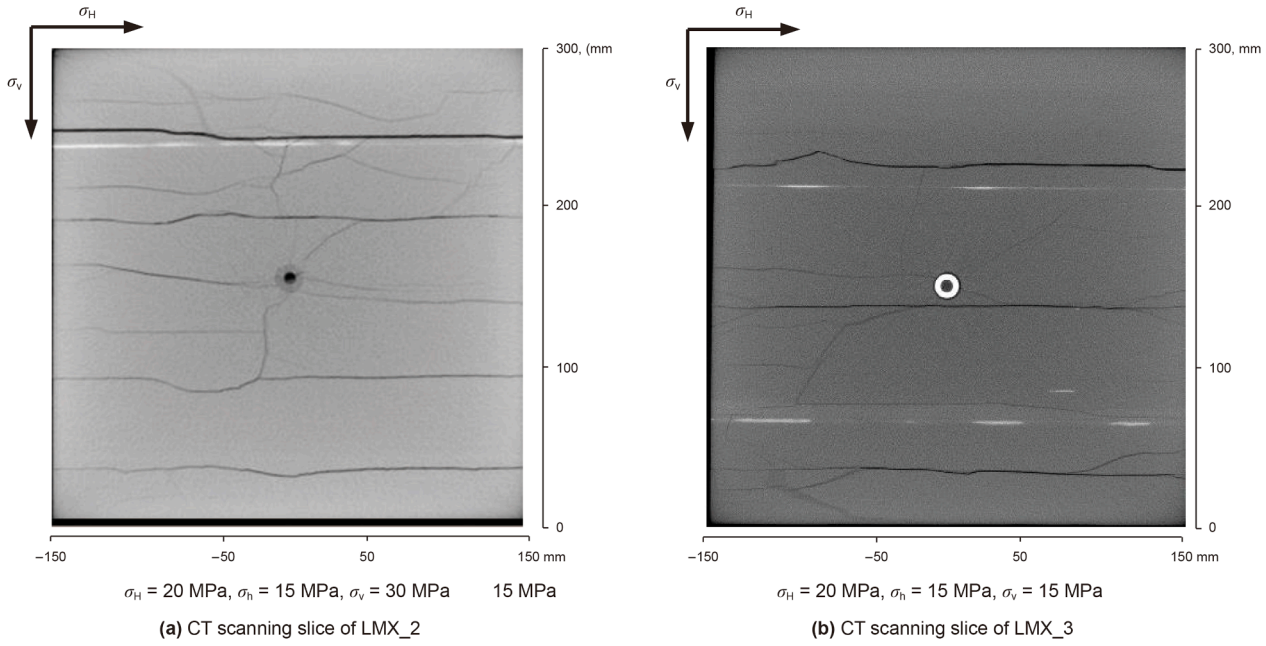

Fig. 4. The CT scanning slice figure (modified from Wu et al. (2019a)).

- The complexity of hydraulic fracture network in tight sandstone is simpler than that in shale.
- The complexity of the fracture network in shale is not constant due to the influence of bedding. It is evident that LMX_2 is more complex than LMX_3 due to a higher vertical loading on bedding.
- The complexity of the fracture network of LMX_SC-CO$_2$ is more complex than LMX_4 due to the low viscosity of SC-CO$_2$, which generates more branched fractures.

3. Results

3.1. Connection model of AE events

Fig. 5 shows the results of the established connection models of C7_1 (top row) and LMX_1 (bottom row). The connection models of other samples are attached in the Appendix. The color of the fractures in Fig. 5 represents the branch number. Fig. 5(a) and (c) are generated using the event-event method (Section 2.1), while Fig. 5(b) and (d) utilize the event-network method (Section 2.1). Although the overall difference between the two methods is insignificant, the event-network method tends to produce a higher number of branches. This occurs because the event-network method allows connections to points beyond just AE event locations, thus increasing branching possibilities. While both methods yield similar overall results, choosing between them may depend on specific research purposes, such as computational efficiency or the need for detailed fracture network complexity. From a modeling perspective, the event-network method demonstrates stronger robustness compared to the event-event method, especially considering the potential errors in AE locations. This is because the event-network method allows for more flexible connections, which can compensate for the inaccuracies of individual AE locations. In both models (Fig. 5), branch-1 fractures, represented by the darkest red, can extend to the boundary, while multi-level branch fractures in lighter red color tend to form in the central area of the rock samples. This branching typically occurs in regions where energy is concentrated. Theoretical studies considering complex fracture criteria, such as the impact of non-inverse-square-root stress singularity on crack propagation criteria, provide additional context for interpreting fracture branching behaviors observed in the connection model (Shen et al., 2024). Since the fracturing fluid spreads from the central area to the boundary, more fracture branching occurs near the center of the sample. It is important to note that the connection model represents the relationships between AE events and does not depict the actual shape of the fractures.

Fig. 6 displays the number of branching in all samples, with solid boxes representing branching using the event-network method and dashed boxes indicating branching using the event-event method. The fracture network in LMX_3 is not complex according to the CT scanning slice (Fig. 4(b)), but its branching

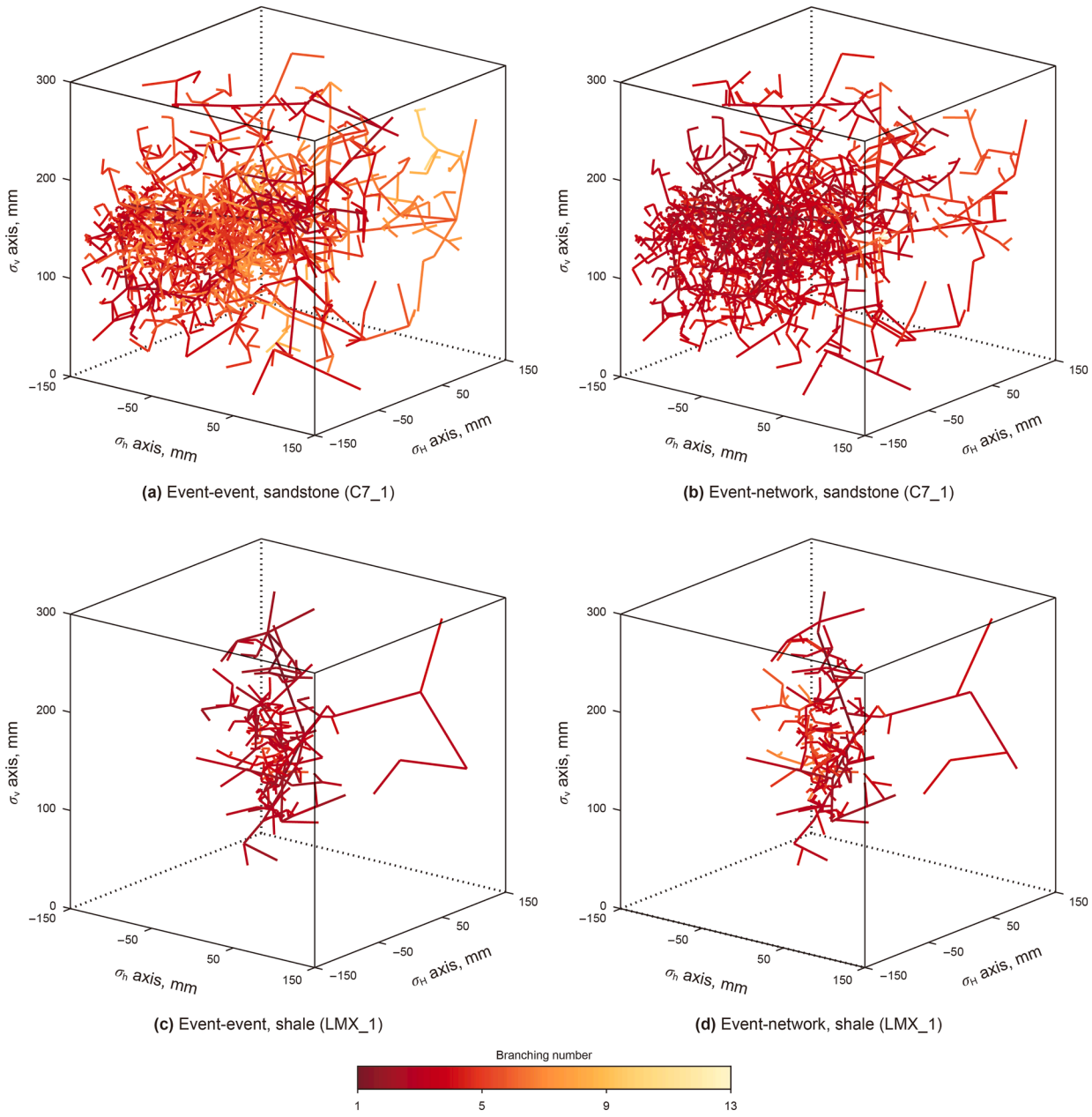

Fig. 5. Left panel: the connected fractures model using the event-event method. Right panel: the connected fractures model using the event-network method. Top row: the results of sample C7_1. Bottom row: the results of sample LMX_1.

number is very high (Fig. 6). Except for LMX_3, the branching numbers in LMX shale are generally lower than that in C7 tight sandstone. LMX_SCO$_2$ has the same branching number as LMX_1. Since branching numbers do not correlate with the superior fracturing effect in LMX_2 compared to LMX_3, nor do they indicate that the fracturing effect in shale is superior to that in sandstone, or that SC-CO$_2$ fracturing is more effective than water fracturing, we conclude that the branching numbers alone cannot reflect the fracturing effect. The branching of fractures may be influenced by local stress changes or lithological variations, and thus does not necessarily represent the overall characteristics of the fracture network.

3.2. Correlation of fractal dimension

We calculate the correlation dimension of the connected fracture models obtained based on the event-event and event-network methods. Fig. 7 shows the results in terms of lg$r$ and lg$C(r)$ relationship for the seven rock samples. The models based on the event-event method typically present a larger fractal dimension compared to the event-network method, as the fracture lengths in the event-network method are generally shorter. Therefore, the presence of more small-scale fractures in the event-event method results in a high value of $C(r)$ in the range of small lg$r$ on the lg$r$ – lg$C(r)$ curve. These curves also show a small growth

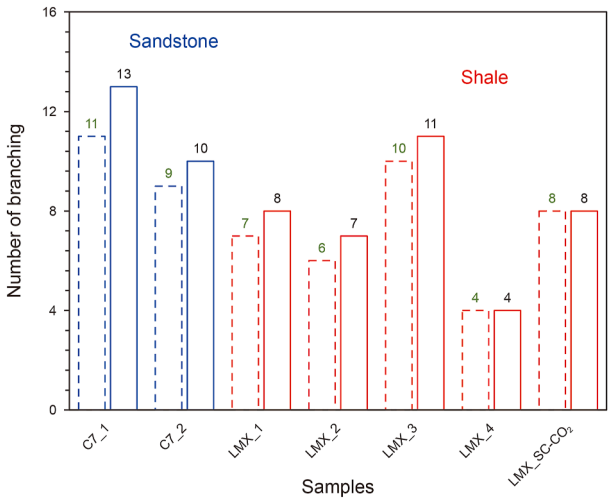

Fig. 6. The number of branching of all the samples.

rate in the large lg$r$ area, which may be due to the boundary effects on fracture propagation limited by the sizes of rock samples. To mitigate the boundary limitation, we fit the lg$r$ – lg$C(r)$ curve in the small lg$r$ area to obtain the slopes as the correlation dimension. All fitted curves have high R^2 (R^2 > 90%, Fig. 7). These results indicate that the lengths of AE links exhibit fractal behavior, and the correlation dimension is a good characteristic feature of fracture networks.

3.3. Tensile-shear ratio of fractures

We use the proportion of tensile-type AE events to represent the tensile-shear properties of each fracture. Since the results from the event-event method exhibit similar characteristics, we only present the tensile-shear properties of fractures based on the event-network method in Fig. 8. We select the first tensile AE event as the initial fracture in the network algorithm of connection models, aligning with the initial tensile-fracture propagation process during hydraulic fracturing. Therefore, the tensile-shear ratio of first-branch fractures is 1 for all the samples. All C7 samples maintain a stable tensile-shear ratio across each branch fracture, whereas the ratio of tensile fractures in LMX samples decreases with an increasing number of branches. This indicates that lithology affects fracture propagation. LMX_SC-CO_2 is a special case, showing an increase in tensile fractures in the terminal branch. This may be because supercritical SC-CO_2 promotes the generation of tensile fractures even in areas far from the injection point due to its high penetration capability in rocks.

4. Discussion

4.1. Correlation dimension of the connected fracture system and fracturing effect

Fig. 9 summarizes the correlation dimensions of all rock samples obtained in Fig. 7. The bars with dashed edges represent the correlation dimensions obtained from the event-event method, while the bars with solid edges represent the correlation dimensions obtained from the event-network method. The correlation dimensions of tight sandstone are lower than those of shale, indicating a higher percentage of short fractures in tight sandstone and more long fractures in shale. This difference may be related to the energy transfer efficiency in different rock types. Being hard and brittle, the shale has a higher energy transfer efficiency, allowing longer fractures to form. Additionally, we observed that the correlation dimension of LMX_2 is greater than that of LMX_3. Li et al. (2018a) discussed that higher vertical stress on the bedding structure can prevent fluid from leaking through the bedding, enhancing the interaction between the bedding and hydraulic fractures. This leads to a more complex fracture network, as observed in LMX_2. The higher correlation dimensions suggest that the fracture network in LMX_2 is more complex than that in LMX_3, which is consistent with previous findings (Fig. 4). In LMX_4, fractured using X-linked guar, only simple fractures are formed near the wellhead, and its correlation dimension is the lowest among all the shale samples (~1.04). The high viscosity of X-linked guar makes it difficult to induce a complex fracture network (Xiong et al., 2018; Zou et al., 2016). On the contrary, the injection of supercritical CO_2 promotes the complexity of the fracture network (Ishida et al., 2021; Zhang et al., 2017a; Zhou and Zhang, 2020), resulting in the highest correlation dimension for LMX_SC-CO_2 among all shale samples.

We recognize that the correlation dimension can reflect the complexity of the fracture propagation process, with a larger correlation dimension indicating a more complex fracture network. A complex fracture network constitutes multi-scale permeability channels, which can enhance oil and gas extraction from multi-scale pore storage spaces. The complex fracture networks also lead to compression of pore spaces at the nanoscale. Recent findings by Huang and Zhao (2023) further suggest that these nanoscale pores interact closely with fracture networks, influencing permeability evolution. The correlation dimension, as a quantitative measure of fractal dimension, effectively characterizes the complexity of fracture networks by reflecting their multi-scale spatial distribution. Higher fractal dimensions indicate that fractures occupy larger effective volumes, forming denser and more intricate networks with numerous branches spanning multiple scales (de Dreuzy et al., 2001; Guo et al., 2015; Wu et al., 2017). Such complexity significantly enhances reservoir permeability, as complex fracture networks provide abundant multi-scale flow pathways, facilitating fluid flow across the reservoir matrix more efficiently compared to simpler, planar fracture structures (Jafari and Babadagli, 2012; Shokri et al., 2016; Zhou et al., 2017). Field observations and numerical simulations have consistently demonstrated that higher fractal dimensions are correlated with increased fluid recovery and stimulated reservoir volumes due to improved connectivity and accessibility to isolated hydrocarbon pockets (Adler et al., 2013; Raterman et al., 2018). Therefore, the correlation dimension serves as a robust proxy for evaluating fracturing effectiveness, directly linking fracture geometry complexity to permeability enhancement. Therefore, a complex fracture network is beneficial for improving the fracturing effect, although there is no direct evidence linking a complex fracture network to a better fracturing outcome. Now we can conclude that the correlation dimension of the connection model effectively reflects the complexity of the fracture network and can be used to evaluate the hydraulic fracturing effectiveness.

4.2. The tensile-shear ratio of fractures and fracturing effect

A higher ratio of tensile fractures is associated with a larger opening degree of fractures, which is beneficial for injecting proppants to maintain fracture permeability. In LMX shales, the ratio of tensile fractures gradually decreases as the number of fracture branches increases, indicating a limited fracturing effect due to lower opening degrees of fractures. However, when fractured with supercritical CO_2, the branch fractures maintain a certain degree of opening. Enhancing the opening degree of

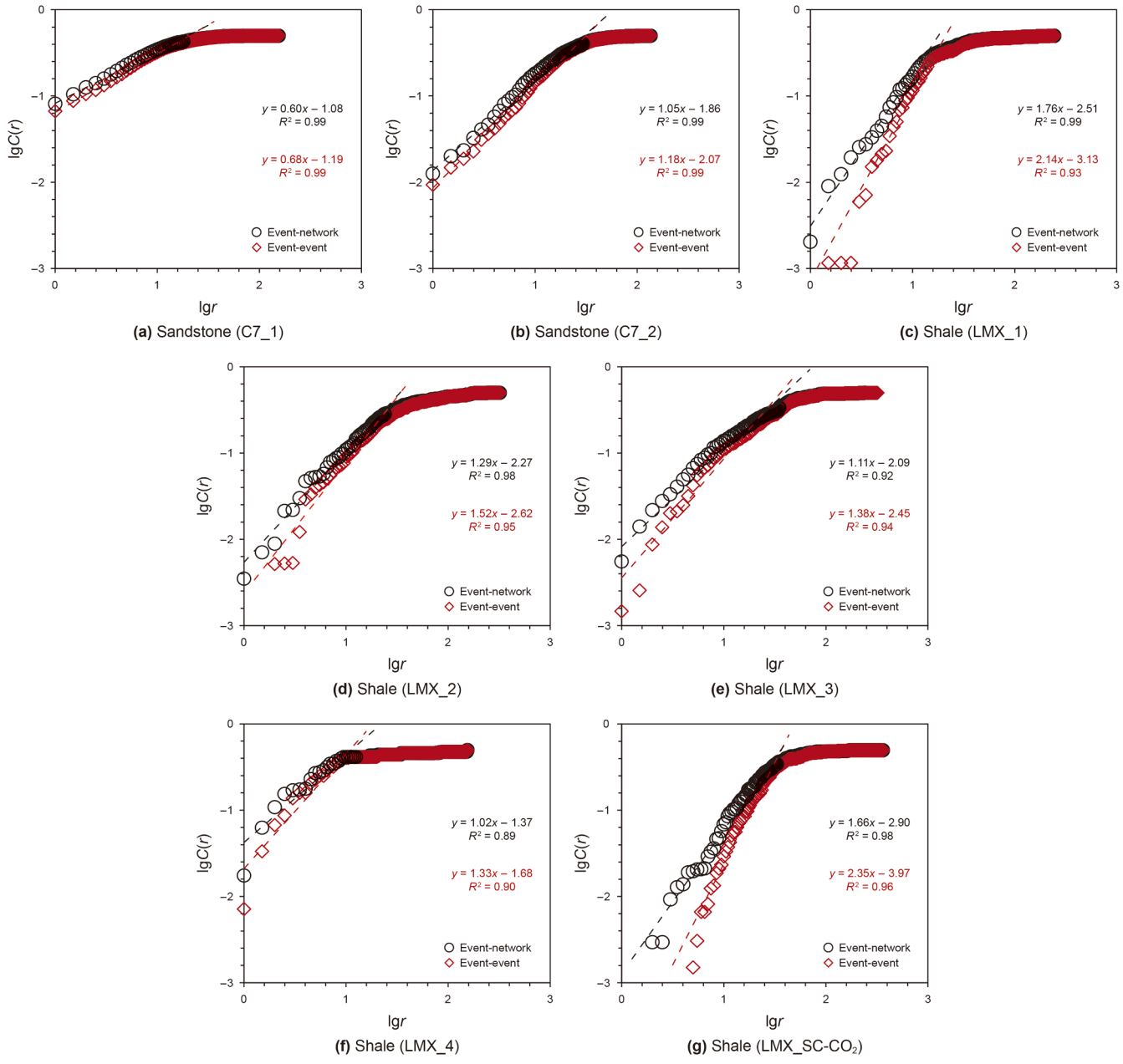

Fig. 7. The correlation dimension of the connected fracture model for the seven rock samples.

fractures in shale may thus improve the fracturing effect. Supercritical CO_2 is effective in this regard, as it can induce complex fractures and increase the opening degree of branch fractures. In contrast, in C7 tight sandstone, the ratio of tensile fractures does not decrease with increasing branches, suggesting that the fractures maintain a consistent opening degree. This may be due to the fluid energy consistently maintained within the fracture networks from the fluid injection point to the boundary. Consequently, although LMX shale exhibits a more intricate fracture system than the tight sandstone, this complexity does not necessarily correlate with higher permeability in the fracture network.

4.3. Sensitivity analysis of AE localization errors on connection model robustness

To enhance the method's robustness evaluation, we conducted a sensitivity analysis by introducing synthetic noise into the AE event locations and evaluating its impact on the branching number and correlation dimension. Considering that localization errors might also affect the moment tensor inversion results (tensile-shear characteristics), Qin et al. (2025) previously discussed this aspect and found that the impact of moderate localization errors on moment tensor outcomes was relatively minor. Given the complexity of fully

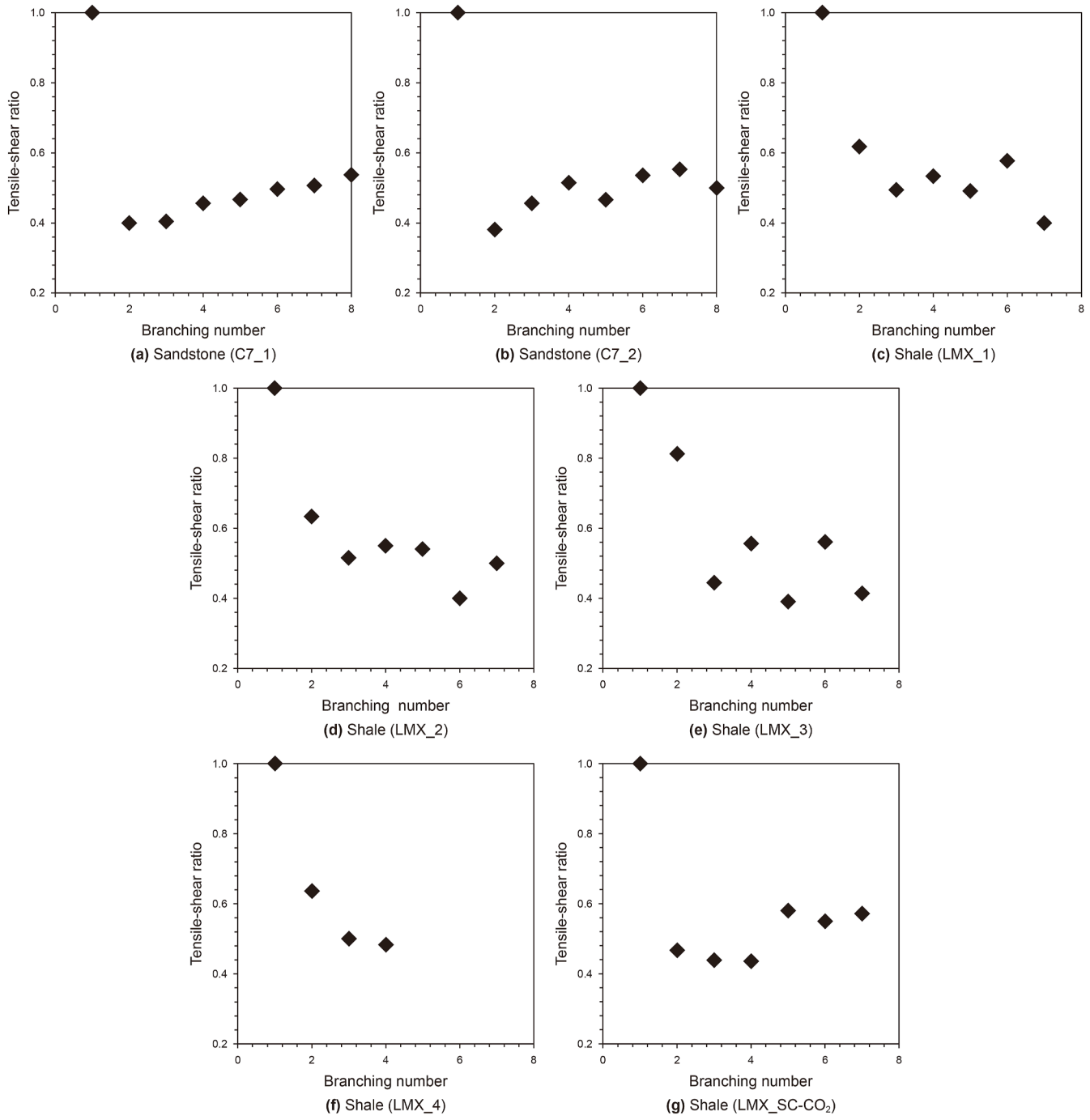

Fig. 8. The tensile and shear ratios of all seven rock samples.

assessing moment tensor sensitivity, our analysis specifically focuses on the branching number and correlation dimension.

We introduced random localization errors in the *x*, *y*, and *z* coordinates of AE events, with maximum error limits set to 6, 12, 18, 24, and 30 mm, corresponding respectively to 2%, 4%, 6%, 8%, and 10% of the sample size (300 mm cubic). For each noise level, calculations for branching number and correlation dimension were repeated 100 times, and the average values were obtained using both the event-event and event-network models. Fig. 10 illustrates the outcomes: (a) branching number under the event-event model for different noise levels, (b) branching number under the event-network model for different noise levels, (c) correlation dimension under the event-event model for different noise levels, (d) correlation dimension under the event-network model for different noise levels. The results indicate that the branching numbers and correlation dimension coefficients are minimally affected by increasing localization errors. Importantly, the rank order among samples remained consistent despite the introduced noise. Notably, the event-network model exhibited greater robustness compared to the event-event model, highlighting its superior reliability in the presence of localization errors.

It is important to acknowledge that our sensitivity analysis considers only randomized synthetic localization errors. Actual

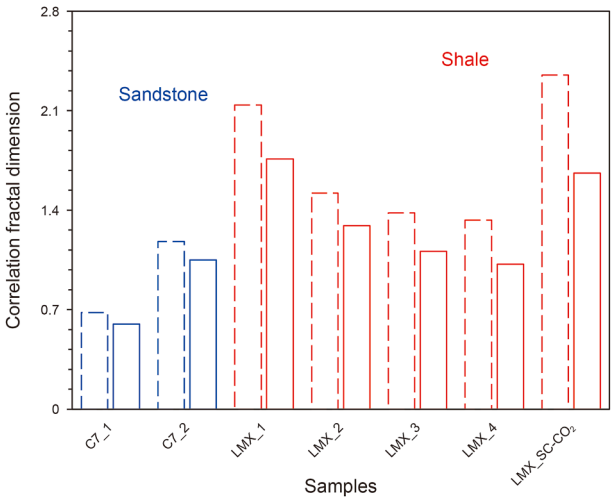

Fig. 9. The value of the correlation fractal dimension of all the samples.

localization results are influenced by multiple complex and heterogeneous factors, making comprehensive quantification challenging. Thus, while we recognize the limitations of our current analysis, we discuss the potential impacts qualitatively and aim to explore more rigorous methods for quantifying sensitivity in future research.

5. Conclusions

We employ a connection method to establish relationships between AE events by incorporating the connectivity between fractures to evaluate the hydraulic fracturing effectiveness in rocks. The application of fracture network complexity and the tensile-shear properties of fractures based on this model is also investigated. The correlation dimension of fracture links within the connection model quantifies the complexity of fracture networks. Additionally, the moment tensor inversion of AE events is used to define the tensile-shear properties of fractures. Based on prior information from fracturing effect evaluations in several experimental datasets, we validate that the correlation dimensions can help quantify the complexity of fracture networks. Higher correlation dimensions in the connection model indicate more complex fracture networks. The tensile-shear ratio of fractures provides valuable information for evaluating permeability enhancement after hydraulic fracturing, which is essential for assessing the fracturing effect. The tensile-shear ratio in the connection model changes with the propagation of fracture branches. Maintaining a high proportion of tensile fractures in each branching leads to a favorable fracturing effect. This AE-based connection model offers a robust evaluation of hydraulic fracturing effectiveness and is particularly valuable in assessing general rock fracturing processes, especially in the formation of complex fracture networks resulting brittle failures.

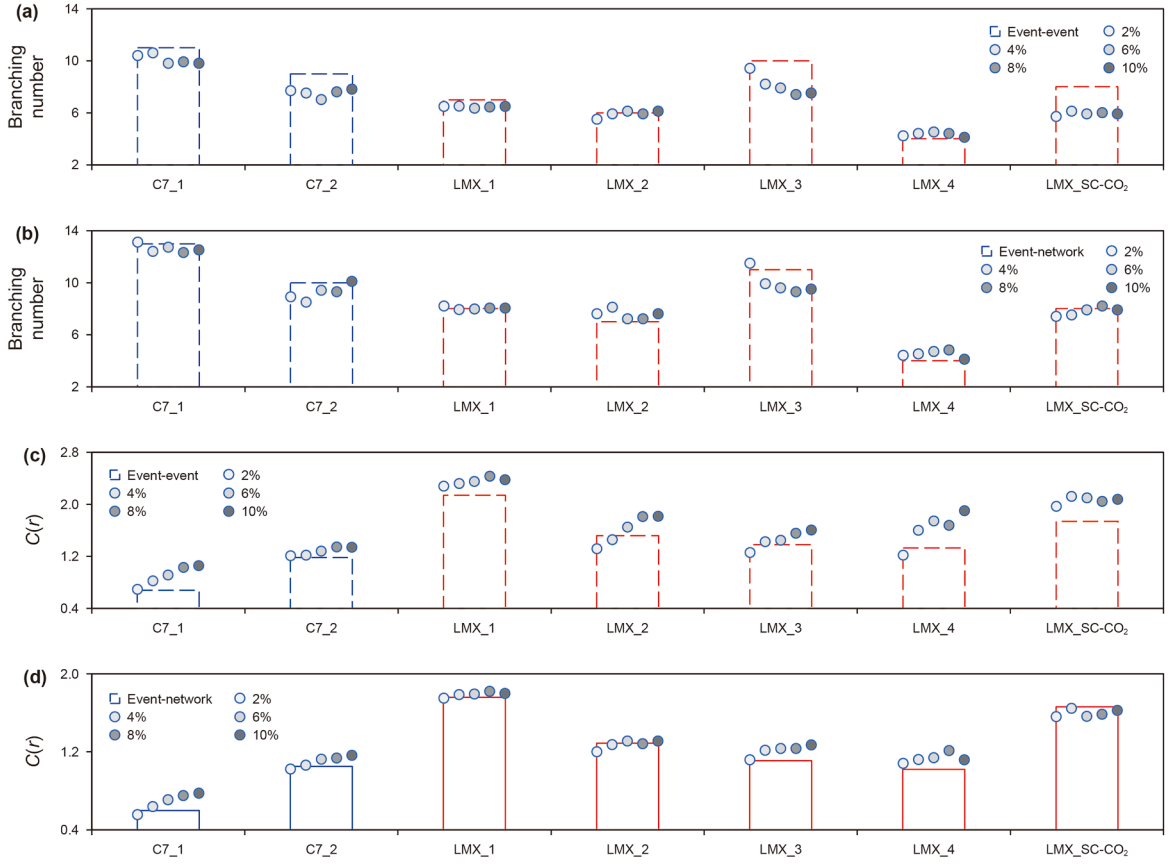

Fig. 10. Sensitivity analysis results: (**a**) branching number under the event-event model, (**b**) branching number under the event-network model, (**c**) correlation dimation under the event-event model, (**d**) correlation dimation under the event-network model, each for varying noise levels.

CRediT authorship contribution statement

Shan Wu: Writing – original draft, Methodology, Investigation, Funding acquisition. **Hong-Kui Ge:** Writing – review & editing, Supervision, Formal analysis, Conceptualization. **Xiao-Qiong Wang:** Validation, Investigation, Conceptualization. **Ke Gao:** Writing – review & editing, Visualization, Investigation, Funding acquisition. **Hai Ding:** Validation, Data curation.

Declaration of competing interest

We declare that there are no conflict of interests. We have no financial and personal relationships with other people or organizations that can inappropriately influence our work.

Acknowledgements

The authors express thanks for financial support from the subprojects of the Natural Science Foundation of China (No. 42302326), the Shenzhen Science and Technology Program (JCYJ20220530113612028), the National Key Research and Development Program of China (Grant No. 2023YFC3707905), and the Fundamental Research Funds for the Central Universities (JZ2025HGTB0191).

Appendix

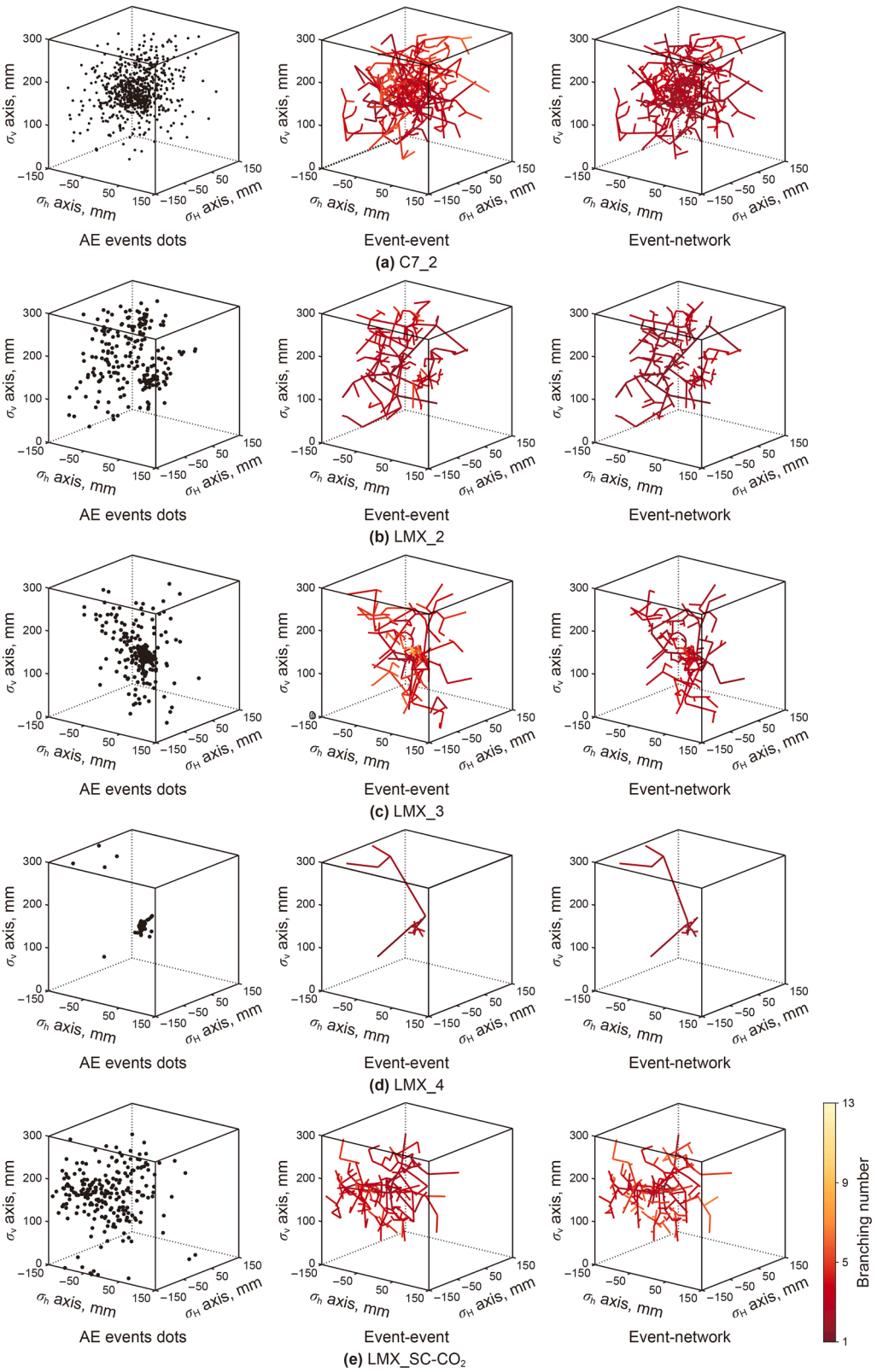

Fig. A1. The connection models of (**a**) C7_2, (**b**) LMX_2, (**c**) LMX_3, (**d**) LMX_4, (**e**) LMX_SC-CO_2.

References

Adler, P., Mourzenko, V., Thovert, J., 2013. Percolation and permeability of heterogeneous fracture networks. In: EGU General Assembly Conference, pp. EGU2013–EGU2543.

Auradou, H., Drazer, G., Hulin, J.P., Koplik, J., 2005. Permeability anisotropy induced by the shear displacement of rough fracture walls. Water Resour. Res. 41, W09423. https://doi.org/10.1029/2005WR003938.

Bennour, Z., Ishida, T., Nagaya, Y., Chen, Y., Nara, Y., Chen, Q., Sekine, K., Nagano, Y., 2015. Crack extension in hydraulic fracturing of shale cores using viscous oil, water, and liquid carbon dioxide. Rock Mech. Rock Eng. 48 (4), 1463–1473. http://10.1007/s00603-015-0774-2.

Chang, S., Lee, C., 2004. Estimation of cracking and damage mechanisms in rock under triaxial compression by moment tensor analysis of acoustic emission. Int. J. Rock Mech. Min. Sci. 41 (7), 1069–1086. http://10.1016/j.ijrmms.2004.04.006.

de Dreuzy, J., Davy, P., Bour, O., 2001. Hydraulic properties of two-dimensional random fracture networks following a power law length distribution: 1. Effective connectivity. Water Resour. Res. 37 (8), 2065–2078. https://doi.org/10.1029/2001WR900011.

Frohlich, C., Davis, S., 1990. Single-link cluster analysis as a method to evaluate spatial and temporal properties of earthquake catalogues. Geophys. J. Int. 100 (1), 19–32. https://doi.org/10.1111/j.1365-246X.1990.tb04564.x.

Gale, J., Elliott, S., Laubach, S., 2018. Hydraulic fractures in core from stimulated reservoirs: core fracture description of HFTs slant core, midland basin, west Texas. In: SPE/AAPG/SEG Unconventional Resources Technology Conference. http://10.15530/urtec-2018-2902624.

Guo, T., Zhang, S., Ge, H., Wang, X., Lei, X., Xiao, B., 2015. A new method for evaluation of fracture network formation capacity of rock. Fuel 140, 778–787. https://doi.org/10.1016/j.fuel.2014.10.017.

Hampton, J., Frash, L., Gutierrez, M., 2013. Investigation of laboratory hydraulic fracture source mechanisms using acoustic emission. In: 47th US Rock Mechanics/Geomechanics Symposium.

Huang, X., Zhao, Y., 2023. Evolution of pore structure and adsorption-desorption in oil shale formation rocks after compression. Energy 278, 127913. https://doi.org/10.1016/j.energy.2023.127913.

Hugot, A., Dulac, J., Gringarten, E., Haouesse, A., 2015. Connecting the dots: microseismic-derived connectivity for estimating volumes in low-permeability reservoirs. In: Unconventional Resources Technology Conference.

Ishida, T., Chen, Q., Mizuta, Y., Roegiers, J., 2004. Influence of fluid viscosity on the hydraulic fracturing mechanism. J. Energy Resour. Technol. 126 (3), 190. http://10.1115/1.1791651.

Ishida, T., Chen, Y., Bennour, Z., Yamashita, H., Inui, S., Nagaya, Y., Naoi, M., Chen, Q., Nakayama, Y., Nagano, Y., 2016. Features of CO_2 fracturing deduced from acoustic emission and microscopy in laboratory experiments. J. Geophys. Res. Solid Earth 121 (11), 8080–8098. http://10.1002/2016JB013365.

Ishida, T., Desaki, S., Kishimoto, Y., Naoi, M., Fujii, H., 2021. Acoustic emission monitoring of hydraulic fracturing using carbon dioxide in a small-scale field experiment. Int. J. Rock Mech. Min. Sci. 141, 104712. https://doi.org/10.1016/j.ijrmms.2021.104712.

Jafari, A., Babadagli, T., 2012. Estimation of equivalent fracture network permeability using fractal and statistical network properties. J. Petrol. Sci. Eng. 92, 110–123. https://doi.org/10.1016/j.petrol.2012.06.007.

Kurths, J., Herzel, H., 1987. An attractor in a solar time series. Phys. Nonlinear Phenom. 25 (1–3), 165–172. https://doi.org/10.1016/0167-2789(87)90099-6.

Lei, X., 2019. Evolution of b-Value and fractal dimension of acoustic emission events during shear rupture of an immature fault in granite. Appl. Sci. 9 (12), 2498. https://doi.org/10.3390/app9122498.

Li, N., Zhang, S., Zou, Y., Ma, X., Wu, S., Zhang, Y., 2018a. Experimental analysis of hydraulic fracture growth and acoustic emission response in a layered formation. Rock Mech. Rock Eng. 51 (4), 1047–1062. https://doi.org/10.1007/s00603-017-1383-z.

Li, N., Zhang, S., Zou, Y., Ma, X., Zhang, Z., Li, S., Chen, M., Sun, Y., 2018b. Acoustic emission response of laboratory hydraulic fracturing in layered shale. Rock Mech. Rock Eng. 51 (11), 3395–3406. https://doi.org/10.1007/s00603-018-1547-5.

Li, Y., Liu, J., Zhao, X., Yang, Y., 2009. Study on b-value and fractal dimension of acoustic emission during rock failure process. Rock Soil Mech. 30 (9), 2559–2563. http://10.3969/j.issn.1000-7598.2009.09.003 (in Chinese).

Liu, Y., Yang, L., Wang, X., Ding, Y., Wang, Y., Zou, Y., 2018. Introduction to the appropriate-stimulation degree of hydraulic fracture networks in shale gas reservoirs. Nat. Gas. Ind. B 5 (1), 29–34. https://doi.org/10.1016/j.ngib.2017.11.005.

Manthei, G., 2005. Characterization of acoustic emission sources in a rock salt specimen under triaxial compression. Bull. Seismol. Soc. Am. 95 (5), 1674–1700. https://doi.org/10.1785/0120040076.

Maxwell, S., 2011. Microseismic hydraulic fracture imaging: the path toward optimizing shale gas production. Lead. Edge 30 (3), 340–346. https://doi.org/10.1190/1.3567266.

Mayerhofer, M.J., Lolon, E., Warpinski, N., Cipolla, C., Walser, D., Rightmire, C., 2010. What is stimulated reservoir volume? SPE Prod. Oper. 25 (1), 89–98. http://10.2118/119890-PA.

Middleton, R., Viswanathan, H., Currier, R., Gupta, R., 2014. CO_2 as a fracturing fluid: potential for commercial-scale shale gas production and CO_2 sequestration. Energy Proc. 63, 7780–7784. https://doi.org/10.1016/j.egypro.2014.11.812.

Ohno, K., Ohtsu, M., 2010. Crack classification in concrete based on acoustic emission. Constr. Build. Mater. 24 (12), 2339–2346. http://10.1016/j.conbuildmat.2010.05.004.

Ohtsu, M., 1991. Simplified moment tensor analysis and unified decomposition of acoustic emission source: application to in situ hydrofracturing test. J. Geophys. Res. Solid Earth 96 (B4), 6211–6221. http://10.1029/90JB02689.

Ohtsu, M., 1995. Acoustic emission theory for moment tensor analysis. Res. Nondestr. Eval. 6 (3), 169–184. https://doi.org/10.1007/BF01606380.

Qin, L., Zha, F., Wu, S., Ding, H., Liu, S., 2025. Acoustic emission inversion for hydraulic fracture geometry with geomechanical constraints. Phys. Fluids 37, 1. https://doi.org/10.1063/5.0245827.

Raterman, K., Farrell, H., Mora, O., Janssen, A., Gomez, G., Busetti, S., McEwen, J., Friehauf, K., Rutherford, J., Reid, R., 2018. Sampling a stimulated rock volume: an Eagle Ford example. SPE Reservoir Eval. Eng. 21 (4), 927–941. https://doi.org/10.2118/191375-PA.

Shen, W., Wu, X., Huang, X., 2024. The effects of non-inverse-square-root stress singularity on some crack propagation criteria in hydraulic fracturing. Acta Mech. Sin. 40 (5), 423246. https://doi.org/10.1007/s10409-023-23246-x.

Shokri, A., Babadagli, T., Jafari, A., 2016. A critical analysis of the relationship between statistical-and fractal-fracture-network characteristics and effective fracture-network permeability. SPE Reservoir Eval. Eng. 19 (3), 494–510. https://doi.org/10.2118/181743-PA.

Taleghani, A.D., Ahmadi, M., Olson, J.E., 2013. Secondary fractures and their potential impacts on hydraulic fractures efficiency. Eff. Sustain. Hyd. Frac. 1–20. http://10.5772/56360.

Wang, J., Ge, H., Wang, X., Shen, Y., Liu, T., Zhang, Y., Meng, F., 2019. Effect of clay and organic matter content on the shear slip properties of shale. J. Geophys. Res. Solid Earth 124 (9), 9505–9525. https://doi.org/10.1029/2018JB016830.

Wang, T., Li, T., Zhao, W., Ma, Y., Chen, Y., 2017. Study on decomposition of acoustic emission signal and identification of rock mass fracture. J. Comput. Methods Sci. Eng. 17, 1–12. http://10.3233/JCM-170757.

Warpinski, N., Mayerhofer, M., Agarwal, K., 2013. Hydraulic fracture geomechanics and microseismic source mechanisms. SPE J. 18 (4), 766–780. http://10.2118/158935-PA.

Wu, S., Ge, H., Wang, X., Meng, F., 2017. Shale failure processes and spatial distribution of fractures obtained by AE monitoring. J. Nat. Gas Sci. Eng. 41, 82–92. https://doi.org/10.1016/j.jngse.2017.02.015.

Wu, S., Li, T., Ge, H., Wang, X., Li, N., Zou, Y., 2019a. Shear-tensile fractures in hydraulic fracturing network of layered shale. J. Petrol. Sci. Eng. 183. http://10.1016/j.petrol.2019.106428.

Wu, S., Li, T., Ge, H., Wang, X., Li, N., Zuo, M., Liu, S., Sun, Y., 2019b. Comparison of the AE monitoring results between the hydraulic fracturing and SC-CO_2 fracturing. In: 53rd US Rock Mechanics/Geomechanics Symposium.

Wu, S., Zhao, Q., Yang, H., Ge, H., 2025. Combining acoustic emission and unsupervised machine learning to investigate microscopic fracturing in tight reservoir rock. Eng. Geol., 107939 https://doi.org/10.1016/j.enggeo.2025.107939.

Xiong, H., Wu, W., Gao, S., 2018. Optimizing well completion design and well spacing with integration of advanced multi-stage fracture modeling & reservoir simulation-A permian basin case study. In: Society of Petroleum Engineers-SPE Hydraulic Fracturing Technology Conference and Exhibition 2018., pp. 1–21. http://10.2118/189855-ms.

Zhang, X., Lu, Y., Tang, J., Zhou, Z., Liao, Y., 2017a. Experimental study on fracture initiation and propagation in shale using supercritical carbon dioxide fracturing. Fuel 190, 370–378. http://10.1016/j.fuel.2016.10.120.

Zhang, Z., Wang, E., Li, N., 2017b. Fractal characteristics of acoustic emission events based on single-link cluster method during uniaxial loading of rock. Chaos Solitons Fractals 104, 298–306. https://doi.org/10.1016/j.chaos.2017.08.028.

Zhou, D., Zhang, G., 2020. A review of mechanisms of induced fractures in SC-CO_2 fracturing. Petrol. Sci. Bullet. 2, 239–253. http://10.3969/j.issn.2096-1693.2020.02.021.

Zhou, Z., Su, Y., Wang, W., Yan, Y., 2017. Application of the fractal geometry theory on fracture network simulation. J. Pet. Explor. Prod. Technol. 7 (2), 487–496. http://10.1007/s13202-016-0268-0.

Zou, Y., Li, N., Ma, X., Zhang, S., Li, S., 2018. Experimental study on the growth behavior of supercritical CO_2 induced fractures in a layered tight sandstone formation. J. Nat. Gas Sci. Eng. 49, 145–156. http://10.1016/j.jngse.2017.11.005.

Zou, Y., Zhang, S., Zhou, T., Zhou, X., Guo, T., 2016. Experimental investigation into hydraulic fracture network propagation in gas shales using CT scanning technology. Rock Mech. Rock Eng. 49 (1), 33–45. http://10.1007/s00603-015-0720-3.